Rudder-Roll Damping Autopilot Robustness to Sway-Yaw-Roll Couplings

Blanke, M.; Christensen, A.C.

Published in:
10th Ship Control Systems Symposium, Ottawa 25-29 Oct. 1993.

Publication date:
1993

Document Version
Tidlig version også kaldet pre-print

RUDDER-ROLL DAMPING AUTOPILOT ROBUSTNESS TO SWAY-YAW-ROLL COUPLINGS

Mogens Blanke[1] and Anders C. Christensen[2]

[1] Dept. of Control Eng. AUC [2]Inst. of Aut. Control Systems, DTH

Ver. 1.1 May 1994

DEPARTMENT OF CONTROL ENGINEERING

Research Report P93-4026 ISSN 0908-1208

This report is an updated version of the paper presented at

10th Ship Control Systems Symposium,
Ottawa, Canada, October 1993

RUDDER-ROLL DAMPING AUTOPILOT ROBUSTNESS TO SWAY-YAW-ROLL COUPLINGS

Mogens Blanke[1] and Anders C. Christensen[2]

[1] Department of Control Engineering, Aalborg University, 9220 Aalborg, Denmark,

[2] Institute of Automatic Control Systems, Technical Univ. of Denmark, 2800 Lyngby, Denmark

ABSTRACT

Roll damping and simultaneous heading control by means of rudders has certain robustness problems. This has been experienced in practice, where a controller performed quite differently on sister ships where the only differences were changes in appendages and loading condition.

Analysis of the rudder-roll damping autopilot problem is difficult, primarily due to its complexity, second because hydrodynamic couplings are sparsely treated in the literature. In this work, symbolic mathematical manipulation is introduced to analyze the hydrodynamic equations and provide relations between hydrodynamic parameters and control dynamics. Based on this, an assessment of structured uncertainty is given that can be used for robust design of RRD/course control systems. The main emphasis is on the effects of coupling terms which have not been thoroughly analyzed before. It is shown that changes in the coupling terms can change the roll damping ability significantly. The effects of uncertainty within given bounds are illustrated on an RRD-course controller using data from a naval multipurpose vessel.. It is shown that realistic changes of coupling terms and other uncertainty can give important changes to linear control dynamics and that these changes can make significant changes to both roll reduction and stability margin.

Contributions of the paper are to advise ways to access the effects of coupling term changes on RRD control, to show the changes in robustness, including roll reduction capability for various parameters, and to provide a complete, parameterized model that can be used for comparison of methodology in RRD design.

Keywords: Rudder-roll damping, Autopilots, Robust Control, Uncertainty Models, Course Control, Automatic Control of Ships.

1. INTRODUCTION

Multivariable control systems that incorporate course control and roll damping by means of rudder (RRD) have become increasingly popular. Reasons include the cost-effectiveness of this approach compared with fin stabilizer solutions and the possibility of applying the RRD concept on existing vessels.

The effectiveness of RRD controls has, however, been debated. Results from full scale evaluation on vessels indicate very satisfactory results showing 50-70 % roll reduction [Blanke et al., 1989], [Källström and Schultz, 1989..]. By contrast, other experiences indicate much less effectiveness in certain cases. A remarkable example has been a series of sister vessels, all equipped with RRD, where the first ship performs very satisfactory, while the roll damping capability was significantly reduced when an identical RRD-course controller was used on the last ship in the series. The hull geometry was not changed, but slight modifications had been made in the form of bilge keels, change of rudder shape, and of loading conditions.

This experience has caused renewed research interest in the robustness properties of multivariable RRD with course control. A key point of interest has been the influence from individual parameters in a mathematical model of sway-yaw-roll. However, due to the very complex nature of the problem at hand, it has only been feasible to analyze it with numerical methods. Assessment of the effects of individual hydrodynamic parameters on a more analytical basis has only been attempted in a few, special cases.

This has changed with the advent and improvements in tools for symbolic manipulation and calculation. Examples are *Mathematica* [Wolfram, 1991]. It has now become manageable to utilize both theoretic results from hydrodynamic theory and experimental experience in a much more direct way in assessment of control system properties [Christensen, 1992]. In particular, it has become feasible to study uncertainty, sensitivity and robustness issues and relate them directly to single model coefficients and physical terms.

This paper focuses on the coupling effects between roll and sway-yaw dynamics which are shown to play an important, yet not widely recognized role in the design of rudder roll damping autopilots.

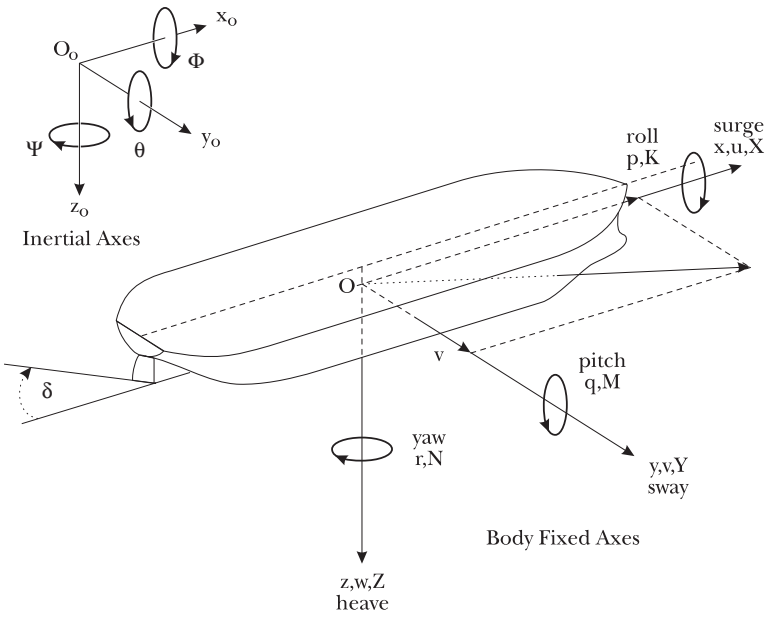

***Figure 1**: Positions, forces and states for a ship, with reference to inertial and ship body fixed coordinate systems. ITTC manoeuvring standard is used: origin is in hull centre of symmetry.*

2. MATHEMATICAL MODELLING

1 illustrates the state definitions and coordinate system for ship movement using the ITTC manoeuvring standard.

2.1 Rudder Generated Motion

The commonplace modelling technique for ship motion is based on the Newtonian equations in surge, sway, yaw, and roll:

$$\begin{aligned} m(\dot{u} - vr - x_G r^2 + z_G pr) &= \sum X \\ m(\dot{v} + ur - z_G \dot{p} + x_G \dot{r}) &= \sum Y \\ I_z \dot{r} + m x_G (ur + \dot{v}) &= \sum N \\ I_x \dot{p} - m z_G (ur + \dot{v}) &= \sum K - \rho g \nabla GZ(\phi) \end{aligned} \tag{1}$$

The last term in the roll equation is the retightening moment: ∇ denotes displacement of the hull, g is the gravity constant, ρ the mass density of water, and GZ the retightening arm. The variables u, v, r, and p are movements of the ship with respect to the principal axes of the body-fixed coordinate system, and X,Y,N, and K the forces and moments along the x and y axes of the body fixed system figure 1. The coordinate (x_G, y_G, z_G) is the position of

the centre of gravity in the ship-fixed coordinate system. In equation (1), we have assumed hull symmetry such that y_G is zero. Forces and moments on the right side of (1) have hydrostatic and -dynamic origin. These terms can be considered linear combinations of nonlinear states and coefficients, which are essentially linear. Write, for example,

$$Y = f\,(u,\dot{u},v,\dot{v},r,\dot{r},\phi,p,|\,p\,|\,p,u^2,r^2,r\,|\,v\,|,rv^2,\ldots) \tag{2}$$

where f is calculated by expanding to a series representation. The terms used in the series are deducted from physical and hydrodynamic considerations combined with experience from model testing:

$$\begin{aligned} Y &= \frac{\partial f}{\partial u}u + \frac{\partial f}{\partial \dot{u}}\dot{u} + \frac{\partial^2 f}{\partial v \partial r}vr + \ldots \\ &\equiv Y_u u + Y_{\dot{u}}\dot{u} + Y_{vr}vr + \ldots \end{aligned} \tag{3}$$

The derivatives in the expansion are referred to as *hydrodynamic coefficients* and the common abbreviated notation Y_u, Y_{uv}, etc. is used. These coefficient sets can be very large with 50-100 coefficients, see [Son & Nomoto,1982].

A nonlinear mathematical model using Newton's laws and the force balance gives, when we use dx/dt for the acceleration vector, E_{nl} for mass-inertia matrix, F_{nl} for the parameter matrix, x_{nl} for the nonlinear state vector, and F_{ext} for lumped, external forces:

$$E_{nl}\frac{dx}{dt} = F_{nl}\,x_{nl} + F_{ext} \tag{4}$$

External forces that depend on states of the system are included in F_{nl}. An example is wind forces, which vary with the ship's heading. This equation is linear in parameters but nonlinear in states. With a nonlinear state vector

$$x_{nl} = [\,|u|v, ur, |v|v, |r|r, |r|v, |v|r, \phi|uv|, \phi u|r|, \phi u|u|, |u|p, p, p|p|, \phi, \phi^3, \delta u|u|\,]^T \tag{5}$$

the parameter and inertia matrices become

$$F_{nl} = \begin{bmatrix} Y_{|u|v} & -m+Y_{ur} & Y_{|v|v} & Y_{|r|r} & Y_{|r|v} & Y_{|v|r} & Y_{\phi|uv|} & Y_{\phi|ur|} & Y_{\phi uu} & Y_{|u|p} & Y_p & Y_{p|p|} & Y_\phi & Y_{\phi\phi\phi} & Y_{\delta uu} \\ N_{|u|v} & N_{|u|r}-m\,x_G & N_{|v|v} & N_{|r|r} & N_{|r|v} & N_{|v|r} & N_{\phi|uv|} & N_{\phi u|r|} & N_{\phi u|u|} & N_{|u|p} & N_p & N_{p|p|} & N_\phi & N_{\phi\phi\phi} & l_{\delta x}Y_{\delta uu} \\ K_{|u|v} & K_{ur}+m\,z_G & K_{|v|v} & K_{|r|r} & K_{|r|v} & K_{|v|r} & K_{\phi|uv|} & K_{\phi|ur|} & K_{\phi uu} & K_{|u|p} & K_p & K_{p|p|} & K_\phi & K_{\phi\phi\phi} & -l_{\delta z}Y_{\delta uu} \end{bmatrix}$$

and

$$E_{nl} = \begin{bmatrix} m-Y_{\dot{v}} & m\,x_G-Y_{\dot{r}} & -m\,z_G-Y_{\dot{p}} \\ m\,x_G-N_{\dot{v}} & I_{zz}-N_{\dot{r}} & -N_{\dot{p}} \\ -m\,z_G-K_{\dot{v}} & -K_{\dot{r}} & I_{xx}-K_{\dot{p}} \end{bmatrix} \tag{6}$$

A linearized model is obtained by defining a linear state vector x and an input vector x_i. In

this paper, we need to include the roll angle φ and the integral of yaw rate ψ in the state vector. The new state vector is $x = [v, r, p, \varphi, \psi]^T$. The inertia matrix must then also be augmented to *E*:

$$E = \begin{bmatrix} E_{nl} & 0 \\ 0 & I \end{bmatrix} \tag{7}$$

The linear model at an arbitrary point of operation is then

$$\dot{x} = E^{-1} F\, x + E^{-1} G\, x_i + E^{-1} F_0 + E^{-1} F_{ext} \tag{7}$$

where the set F, G are:

$$\begin{aligned} [F, G] &= F_{nl}\left[\frac{\partial x_{nl}}{\partial x}, \frac{\partial x_{nl}}{\partial x_i}\right]_{x_0,\, x_{i,0}} \\ F_0 &= F_{nl}\, x_{nl}\big|_{x_0,\, x_{i,0}} \end{aligned} \tag{8}$$

This linearization is easily calculated in symbolic form to show explicit parameter dependencies. As an example, the F and G matrices are, at ship speed U and an equilibrium point $[v_0, r_0, p_0, \varphi_0, \psi_0] = [0,0,0,0,0]$:

$$F = \begin{bmatrix} UY_{uv} & U(-m + Y_{ur}) & Y_p + UY_{up} & Y_\Phi + U^2 Y_{\Phi uu} & 0 \\ UN_{uv} & U(N_{ur} - m\, x_G) & N_p + UN_{up} & N_\phi + U^2 N_{\Phi uu} & 0 \\ UK_{uv} & U(K_{ur} + m\, z_G) & K_p + UK_{up} & -gm\, GM + U^2 K_{\Phi uu} & 0 \\ 0 & 0 & 1 & 0 & 0 \\ 0 & 1 & 0 & 0 & 0 \end{bmatrix} \tag{9}$$

$$G = \begin{bmatrix} U^2 Y_{\delta uu} \\ l_{\delta x} U^2 Y_{\delta uu} \\ -l_{\delta z} U^2 Y_{\delta uu} \\ 0 \\ 0 \end{bmatrix} \tag{10}$$

The coefficients in the F and G matrices clearly show the dependence of ship speed. In the G matrix, rudder forces cause the square law variation in speed. In the (v,r) upper left corner of the F matrix, the steering part, elements vary linear with speed. In the (p, φ) part, the roll part, elements are only slightly affected by speed. The integration to heading angle, ψ, is speed independent. The E matrix has no speed dependent elements, and has diagonal dominance. Hence, multiplication by its inverse does not change this overall picture. These basic relations between parameters in the equations of motion and ship speed are essential for the baseline design of autopilots and rudder-roll damping controllers.

2.2 Wave Generated Motion

Wave disturbances cannot be modelled as forces and moments in the F_{ext} vector in (9). The

reason is that wave forces act over the entire hull. Instead of integrating through the hydrodynamic equations above, wave induced motions are calculated as response functions from strip theory. The result is that wave disturbances are characterized in a vector $x_w = [v,r,p,\varphi,\psi]_w$. The differential equations describing the relation between wave height, ς_w, and hull motions in x_w are complex because the A_w and B_w matrix elements depend on wave length, λ, wave direction, χ, and encounter frequency, ω_e:

$$\dot{x}_w = A_w(\lambda,\chi,\omega_e)\,x_w + B_w(\lambda,\chi,\omega_e)\,\zeta_w \tag{11}$$

The solution to (12) can be found experimentally or calculated by strip theory methods by numerical integration of wave forces over the ship's entire hull. Strip theory is essentially linear, and we can also assume that the motion if the hull is a superposition of the wave induced motion and that created by rudder activity.

Therefore, the motion resulting from the combined action of waves (x_w), rudder (x_i), and other external forces (F_{ext}) must be calculated as the sum of the states x(t) and x_w(t). This combined state output vector is denoted z(t). The mathematical model for the part of the system to be controlled is then the 5th order state space equation for x(t) with waves considered as an output disturbance:

$$\begin{aligned} \dot{x} &= E^{-1}F\,x + E^{-1}G\,x_i + E^{-1}F_{ext} \\ z &= x + x_w \end{aligned} \tag{12}$$

Investigation of the effects of changes in the parameters of the matrices E, F and G is thus a natural point to start a sensitivity and robustness analysis.

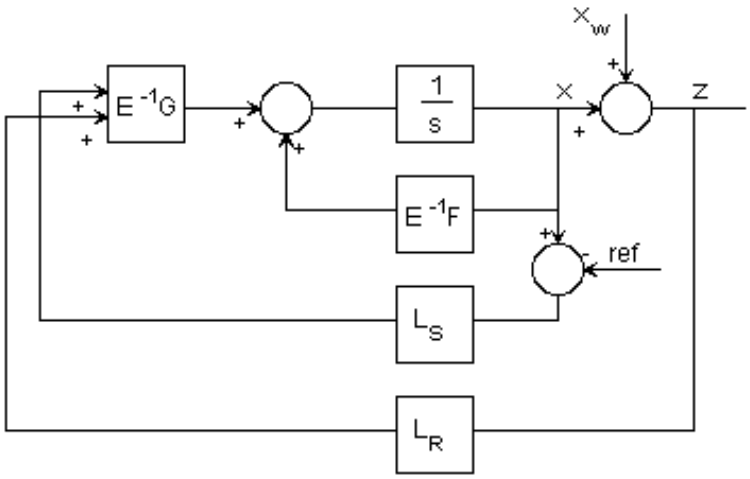

Figure 2 *Idealized control system structure. L_S is undisturbed state feedback from steering, L_R is feedback from the combined wave and hull motion states.*

3. HEADING CONTROL WITH RUDDER-ROLL DAMPING

The main objective in roll damping is to minimize the wave impact on ship motions, expressed as the p and φ components of z. In heading control, the main objective is to maintain the average heading while responding as little as possible to first order wave motions in v, r, and ψ. The latter is a consequence of a desire to obtain minimal propulsion losses from steering. The mean squares of motion values with and without control are hence adequate measures of control quality in waves for both control tasks. In addition to properties in waves, overall stability requirements need to be looked into in the course of designing a controller.

3.1 Basic Controller Design

With a closed loop control, the input signal x_i is determined by a reference value and the measured quantity. If proportional state feedback is used, assuming feedback L_R from an ideal reconstruction of the state vector x(t) and feedback L_R from the wave disturbed state vector z(t):

$$\begin{aligned} \dot{x}(t) &= E^{-1} F\, x(t) + E^{-1} G\, x_i(t) + E^{-1} F_{ext}(t) \\ z(t) &= x(t) + x_w(t) \\ x_i(t) &= -L_S\,(x(t) - x_{ref}(t)) - L_R\, z(t) \end{aligned} \tag{13}$$

The state equation for the closed loop control system is then

$$\begin{aligned} \dot{x}(t) = &(E^{-1}F - E^{-1}G\,(L_R + L_S)\,)\, x(t) - E^{-1}G L_R\, x_w(t) \\ &+ E^{-1}G L_S\, x_{ref}(t) + E^{-1} F_{ext}(t) \end{aligned} \tag{14}$$

$$z(t) = x(t) + x_w(t)$$

and the response functions associated with x_{ref} and x_w are

$$\begin{aligned} x(s) = &[sI - (E^{-1}F - E^{-1}G\,(L_R + L_S)\,)]^{-1} E^{-1}G L_S\, x_{ref}(s) \\ &- [sI - (E^{-1}F - E^{-1}G\,(L_R + L_S)\,)]^{-1} E^{-1}G L_R\, x_w(s) \end{aligned} \tag{15}$$

In the heading control loop, rudder motion due to first order wave motion is undesired. A Kalman filter or a nonlinear observer is therefore used to reconstruct the undisturbed state vector, x(t). In the roll damping part of a controller, roll components of $x_w(t)$ are needed. [Blanke et.al, 1989]. Therefore, we can use a nominal controller where L_S takes feedback from undisturbed states in yaw-sway (x(t)), L_R takes feedback from actual motion components in roll (z(t)). This is illustrated in figure 2, where the reference vector for yaw rate and yaw angle ($x_{ref}(t)$) is also shown.

When considering speed dependency of elements in the F and G matrices, it is obviously advantageous to take account of speed variation in an explicit way. Gain scheduling is therefore employed on the L_R and L_S matrices. When applying gain scheduling, it is wise to

consider the elementary physics of a ship, since a controller does not have the forces available to make any dramatic changes to natural behaviour. The speed dependence found in the (E^{-1} F) matrix should therefore be the same as that of the closed loop ($E^{-1}F$ - $E^{-1}G(L_R+L_S)$). This can be achieved with the following gain scheduling, where U_d is a nominal value used for the design, and U_0 is actual average speed:

$$L_S = \left(0, -l_r \left(\frac{U_d}{U_0} \right), 0, 0, -l_\psi \right)$$
$$L_R = \left(0, 0, -l_p \left(\frac{U_d}{U_0} \right)^2, -l_\phi \left(\frac{U_d}{U_0} \right)^2, 0 \right) \qquad (16)$$

The transferfunctions from rudder to yaw rate and from rudder to roll angle are illustrative for the control task. They are calculated as shown in (16). Figures 3 and 4 show these functions for a multipurpose naval vessel. The transfer functions show the well known non-minimum phase nature in the rudder to roll part, and some effect of cross coupling sway-yaw-roll is seen in the rudder to yaw-rate curve. Figure 3 also shows the Bode plot for the closed loop yaw-rate reference to yaw-rate. This curve has a zero at zero frequency due to heading angle feedback.

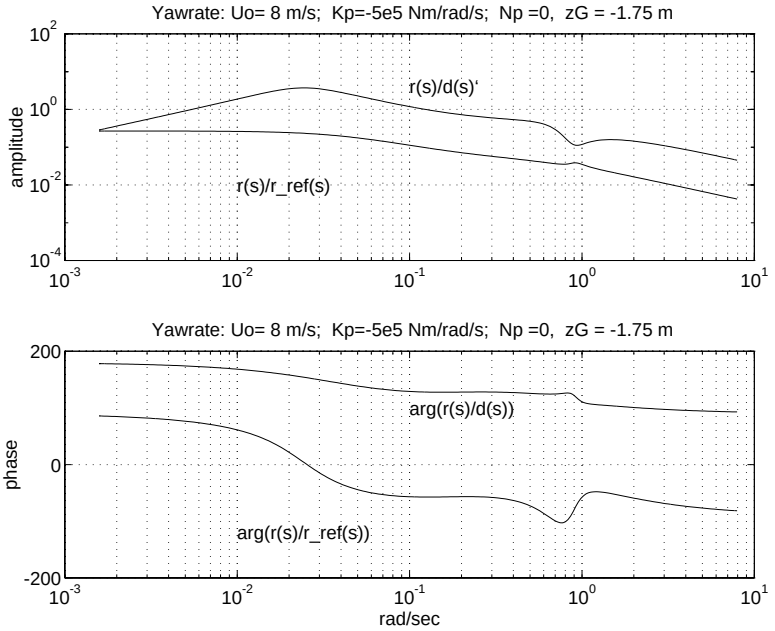

Figure 3 *Yaw-rate transfer functions: r(s)/d(s) in open loop; $r(s)/r_{ref}(s)$ in closed loop. The closed loop has a zero in zero due heading angle feedback.*

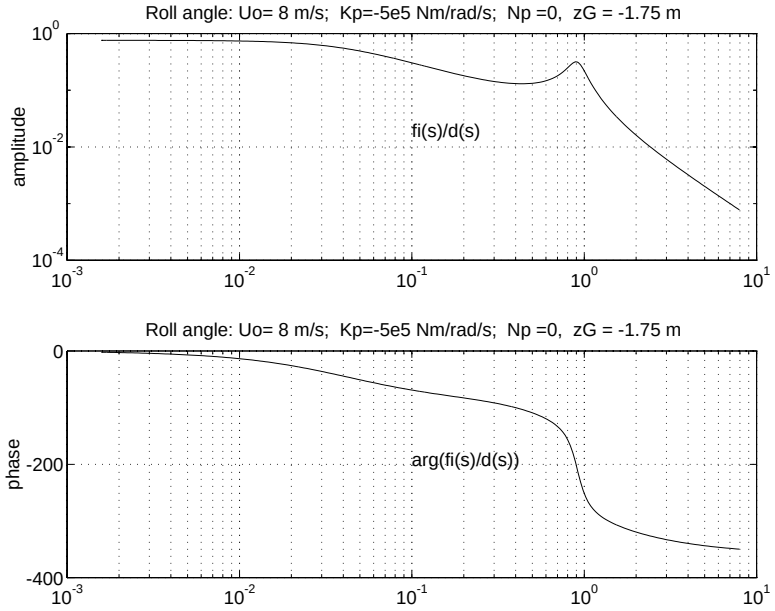

Figure 4*: Roll from rudder transfer function. Note that one transfer function zero is in the right half plane.*

3.2 Performance in Waves

The reduction ratio function, |rr|, is a key indicator for control quality in waves since it expresses the ratio between motion with control and motion without control. When RRD is combined with heading control, the roll damping capability has major emphasis. The |rr| functions for roll damping are therefore the most interesting in this context.

The mean square of the i´th component of the motion vector z(t) is determined by the powerspectrum of wave amplitude, $G_{\zeta\zeta}$ and the wave response operator, $WRO_{x\zeta}$ as shown in equation 15, where the reduction ratio is also calculated.

$$E\{z_i^2(t)\} = \frac{1}{\pi}\int_0^\infty \left|\frac{z_i(\omega_e)}{x_{wi}(\omega_e)}\right|^2 |WRO_{x,\zeta}(\omega)|_i^2 \, G_{\zeta\zeta}(\omega)\, d\omega \quad i = 1,2,...,5$$

$$rr_i(\omega_e) = \left[\frac{z_i(\omega_e)}{x_{wi}(\omega_e)}\right] \quad i = 1,2,...,5 \qquad (17)$$

Here, ω is wave frequency and ω_e is encounter frequency. Details can be found, e.g., in [Blanke, 1982]. Efficient roll damping is obtained when $|rr_p|$ and $|rr_\varphi|$ are well below 1 over the range of frequencies considered. Requirements to roll damping performance are often specified in terms of the shape of the $|rr(\omega_e)|$ function at different values of ship speed and a maximum value of wave height. Robust control is achieved if the required value of $|rr(\omega_e)|$

is met regardless of changes in ship speed, loading conditions, hydrodynamic parameters or other coefficients in the equations of motion.

For a roll damping system, the key measure of effectiveness is the roll reduction ratio, |rr|. One informative measure for the roll rate motion reduction, expressed in the frequency domain, is:

$$rr_{\phi}(j\omega) = \left[\frac{|\phi(s) + \phi_w(s)|_{with\ control}}{|\phi(s) + \phi_w(s)|_{open\ loop}} \right]_{s=j\omega} \tag{18}$$

Another is the measure one would use on time series data:

$$RR_{\phi} = \left[\frac{Var(\phi)_{with\ control}}{Var(\phi)_{open\ loop}} \right] \tag{19}$$

$$with \quad Var(\phi) = E\{(\phi(t) + \phi_w(t))^2\} - (E\{\phi(t) + \phi_w(t)\})^2]$$

Calculation of the |rr| ratio requires calculation of

$$x(s) + x_w(s) = (I + [sI - (E^{-1}F - E^{-1}G(L_R + L_S))]^{-1} E^{-1}GL_R)\, x_w(s) \tag{20}$$

These quantities are used in the following to assess the effects of parameter sensitivity on closed loop performance. The couplings between roll and yaw-sway are particularly interesting and have not been subject to detailed investigations before.

The results of a nominal design, where parameters are given in table 2, are plotted in figure 5. The two curves shown are the $|rr_p|$ and the $|rr_{\varphi}|$ ratios. In a seaway, waves will generate roll motion in both p and φ. Assessment of total performance will therefore require the wave response operators for both p and φ with the representation chosen here.

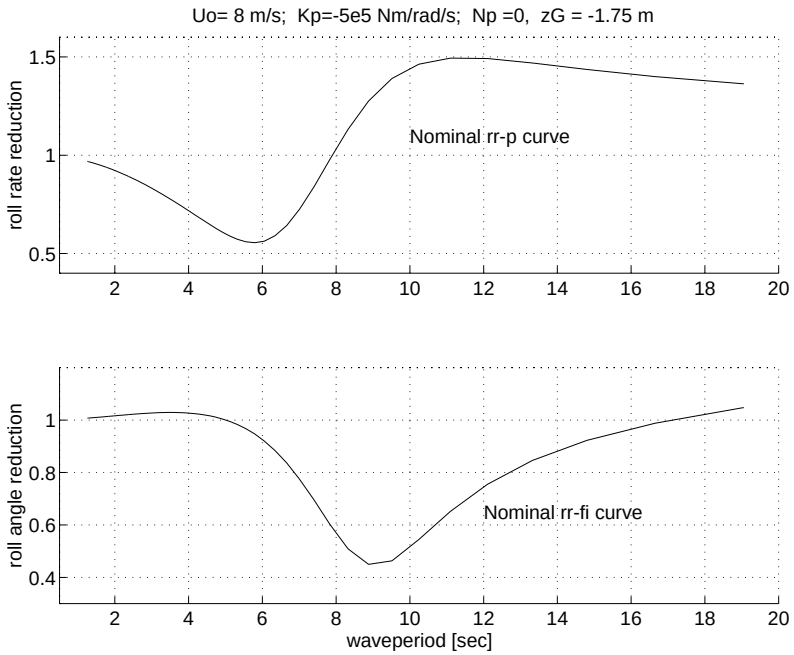

Figure 5 *Rol-reduction for roll rate and roll angle. Nominal values for the controller were chosen.*

3.3 Multipurpose Naval Vessel

The robustness issues raised are illustrated by using a multipurpose naval vessel as an example [Blanke, et.al., 1989]. The data listed in tables 3 and 4 were obtained at the project state and are estimated by the Danish Maritime Institute, DMI. The data are not based on model tests.

From data in the tables, rudder force is estimated as

$$Y(\delta) = \frac{1}{2}\rho C_L A_{rudder} U_0^2 \sin\left(\frac{\pi}{2}\frac{\delta}{\delta_{stall}}\right)$$
$$Y(\delta) \_ Y_\delta \delta = \frac{1}{2}\rho \frac{\pi C_L}{2\delta_{stall}} A_{rudder} U_0^2 \delta \qquad (21)$$

The System matrices $E^{-1}F$ and $E^{-1}G$ are, with $U_0 = 9$ m/s:

$$E^{-1}F = \begin{bmatrix} -0.1787 & -0.7336 & 0.2071 & 0.9102 & 0 \\ -0.0183 & -0.5250 & 0.0058 & 0.0151 & 0 \\ 0.0342 & -1.5153 & -0.1697 & -0.7502 & 0 \\ 0 & 0 & 1 & 0 & 0 \\ 0 & 1 & 0 & 0 & 0 \end{bmatrix}$$

(22)

$$E^{-1}G = \begin{bmatrix} 0.2053 \\ -0.0338 \\ -0.0465 \\ 0 \\ 0 \end{bmatrix}$$

A controller was designed with adequate stability margin and a roll angle reduction ration of 0.5 around the ship's natural roll eigenfrequency. The controller parameters are listed in table 1.

Table 1 Parameters for Nominal Controller

U_d	10	m/s
L_r	6.75	rad/(rad/s)
L_φ	3.38	rad/rad
L_r	9.75	rad/(rad/s)
L_ψ	0.06	rad/rad

When designing an RRD autopilot, the linear system properties are not the only important issues. Rudder speed saturation is a nonlinear phenomenon of major importance [van Amerongen et.al, 1987], [Källström & Schultz, 1989], [Blanke et.al, 1989]. However, the performance of the system will never become better than the linear design. Basic stability, sensitivity, and robustness properties must therefore primarily be investigated in the linear domain.

The controller used for illustration is quite idealized. In a real RRD autopilot design, Kalman filtering will be applied for state reconstruction. When model uncertainties are present in a controller with state reconstruction, sensitivity to model errors is much higher than the results presented here. This investigation is therefore an estimate of the minimal influence that parameter changes will have on a real RRD autopilot.

4. ROLL-SWAY-YAW COUPLINGS

The coupling between the sway, yaw and roll states are determined by the elements of the state matrix $E^{-1}F$. The expressions for this product is too long to be directly useful, see Appendix A where E^{-1} is expanded for reference. One can observe, however, that couplings occur mainly through the elements in F, and not so much through the E^{-1} matrix. The significance and magnitude of coupling effects can therefore be assessed from a scrutiny of the hydrodynamic coefficients involved at the {31, 32, 13, 23, 14, and 24} positions of the F matrix:

$$F_{coupling} = \begin{bmatrix} . & . & Y_p + U\,Y_{up} & Y_q + U^2\,Y_{quu} & . \\ . & . & N_p + U\,N_{up} & N_q + U^2\,N_{quu} & . \\ U\,K_{uv} & U\,(K_{ur} + m\,z_G) & . & . & 0 \\ 0 & 0 & . & . & 0 \\ . & . & 0 & 0 & . \end{bmatrix} \tag{23}$$

This means that 6 terms shall be investigated. In contrast to manoeuvring coefficients, roll couplings have not been thoroughly investigated, and the only published results are from [Son & Nomoto, 1982] and [Källström & Schultz, 89]. There is therefore not a large base of experience to draw at. However, some insight can be gained through considering the physics that create the individual coefficients. For some of

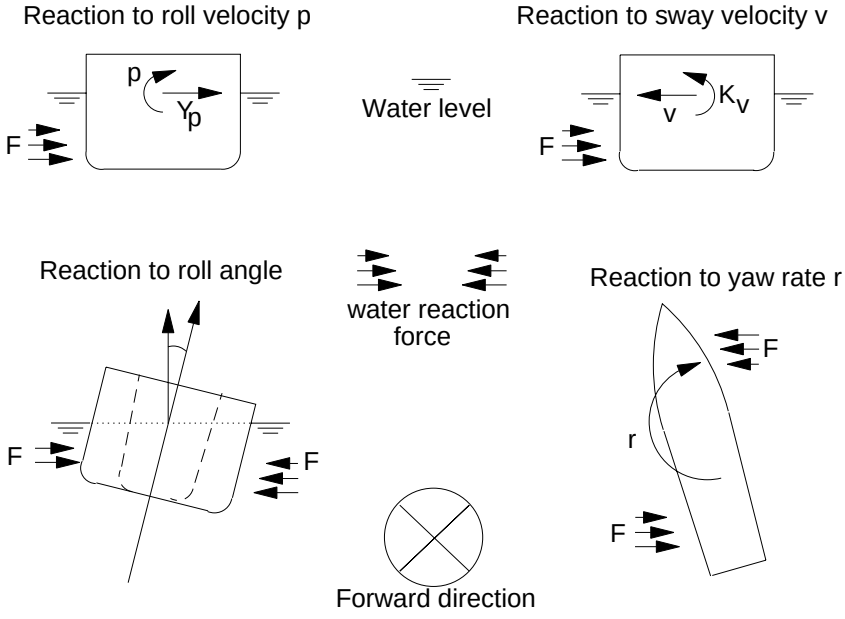

***Figure 6**: Coefficient diagrams for evaluating coupling coefficients between yaw, sway and roll states.*

the hydrodynamic terms, sign and size can be assessed by *coefficient diagrams* shown in figure 6, see f.ex. (Comstock, 1967). Other parameters can be quantified through geometric considerations, as illustrated in figure 7.

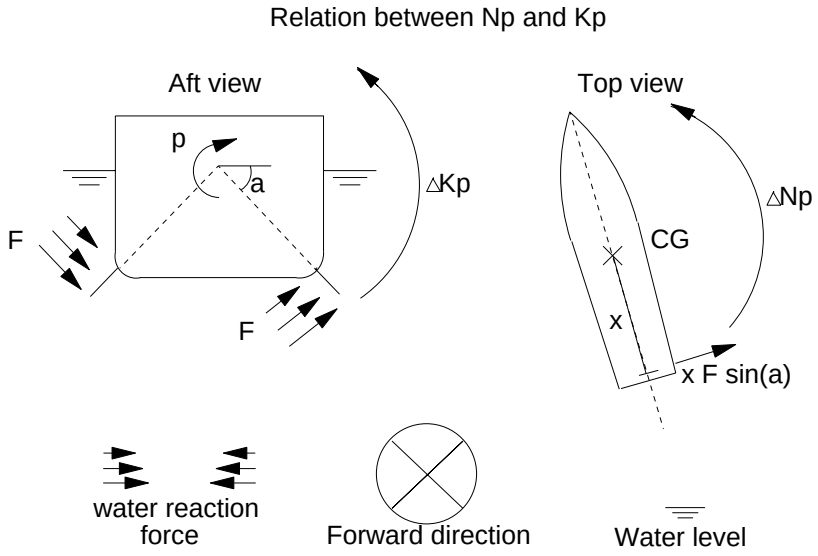

***Figure** 7: Illustration of the relationship between K_p, Y_p, and N_p. A bilge keel is placed at a distance x from the origin at an angle a to horizontal.*

Roll moment from roll velocity K_p, K_{up}. The roll velocity in itself gives a frictional force $K_{|p|p}|p|p$, damping the roll motion. Most literature uses a K_p and/or a K_{up} tem for the roll damping. The occurrence of this term can be explained from non-ideal viscous fluid phenomena, including lift forces from appendages. It can also be seen as an approximation to the $K_{|p|p}$ $|p|p$ term since, if $p=p_0\sin(\omega t)$,

$$| p | p = + 0.849\, p \tag{24}$$

The size of this coefficient depends primarily on the wetted surface, roughness of the hull and the shape and size of appendages. The sign of both sway and roll coefficients of this force are negative. The magnitude of K_p can be determined from experience data for damping of roll motion.

The roll of a ship is easily characterized by natural roll frequency ω_0 and the damping ζ of a rudder induced roll motion. Using a standard notation where K is external roll moment, and ignoring roll coupling to other motions, we get:

$$\phi(s) = \frac{1}{s^2 + 2\zeta\omega_0 s + \omega_0^2} \; \frac{K(s)}{I_{xx} - K_{\dot{p}}} \tag{25}$$

The damping coefficient and natural roll eigenfrequency are:

$$\zeta = \frac{1}{2} \frac{K_p + U\, K_{up}}{\sqrt{\rho \Delta g\, GM\, (I_{xx} - K_{\dot{p}})}}$$

$$\omega_0 = \sqrt{\frac{\rho \Delta g\, GM}{(I_{xx} - K_{\dot{p}})}} \tag{26}$$

The inertias I_{xx} and added inertia K_{pdot} can be estimated as follows:

$$I_{xx} = \rho\, \Delta \left(0.3\, B\right)^2$$

$$K_{\dot{p}} = 0.2\, \rho\, \Delta \left(\frac{1.05\, B}{2}\right)^2 \tag{27}$$

Then the linear roll damping is given by:

$$K_p + U\, K_{up} = 0.762\, \zeta(U)\, \rho\, \Delta\, B \sqrt{g\, GM} \tag{28}$$

If large amplitudes of roll are used to determine the damping, a harmonic linearization (25) of the $K_{p|p|}$ p|p| term should be used to get a correct result.

Roll moment from sway velocity K_{uv}, The top right diagram in figure 5 illustrates the behaviour with a negative sway velocity of the ship. The Y_{uv} uv force produces a large roll moment because the pressure centre is located well below the CG and the coordinate origin. A negative sway velocity will produce a negative roll moment. The centre of pressure is usually located about 35% of the draft, D, below the water surface. Therefore

$$K_{uv} = -0.35\, D\, Y_{uv} \tag{29}$$

Roll moment from yaw rate (K_{ur} + mz_G). The K_{ur} term depends on fore-aft symmetry. Due to appendages of the aft part of the hull, K_{ur} is expected to be negative. The centre of gravity coordinates x_G, z_G plays a more significant role. The centre of gravity can easily move with the loading condition of the ship. Ship´s officers keep control with the ship stability through the metacentric height GM. This means z_G can vary with the consequence that coupling terms may change significantly.

Yaw moment and sway force from roll rate N_p, N_{up}. Y_p, Y_{up}. The yaw coefficients N_p and N_{up} relate to fore/aft asymmetry of the ship. Comparing to the bottom right sketch in figure 2, showing a right turn, it is seen, that the size and sign of these coefficients is significantly dependant on the trim angle of the ship. By lowering one end of the ship and lifting the other transfers wetted surface area from one side of the CG to the other (in the x axis direction). Trimming front down, the coefficients are increased in positive direction, and negative for aft trim. The sign and size of these coefficients are difficult to say much about, and an absolute value depends on the hull form.

However, when part of the damping is obtained by adding bilge keels or other appendages

onto a hull design, the change in N_p and Y_p relate directly to the increase in K_p through the position of the appendages. This is illustrated in figure 3. The bilge keel in the figure is situated at an angle (a) to horizontal and the moment arm is approximately ½B. The drag force is assumed perpendicular to this direction. The force and moments are hence

$$\partial K_p(x)\; p \cong \frac{B}{2}\,\partial L(x) \qquad (\forall x : \partial K_p(x) < 0)$$

$$\Delta K_p = \int_{x_1}^{x_2} \partial K_p(x)\, dx$$

$$\Delta Y_p = -\int_{x_1}^{x_2} \partial K_p(x)\, \frac{2\sin(a)}{B}\, dx \qquad (30)$$

$$\Delta N_p = \int_{x_1}^{x_2} x\, \partial K_p(x)\, \frac{2\sin(a)}{B}\, dx$$

It should be noted, that the force´s arm should be modified from ½B to the actual in certain cases, e.g., when a rudder contributes significantly. As an example, if damping is changed by ΔK_p by adding a bilge keel from 0 to $-¼L_{pp}$, and ΔK_p is uniform along the keel, then obviously,

$$\Delta Y_p \cong -\frac{2\sin(a)}{B}\,\Delta K_p$$

$$\Delta N_p \_ \sin(a)\,\frac{L_{pp}}{4\,B}\,\Delta K_p \qquad (31)$$

A typical increase in ζ is from 0,1 to 0,25. Then, calculation of the K_p, Y_p, and N_p terms follow from 28 and 30.

Yaw and sway from roll angle, N_φ and Y_φ: The bottom left diagram in figure 2 illustrates the hull in a negative roll position. The yaw and sway coefficients N_φ and Y_φ are difficult to say anything about, other than that they are small. The effect of these coefficients has been discussed by Eda [(Eda,1980] as being a result of a *hull-camberline effect*. The hull-camberline is basically the symmetry line of the geometrical shape constructed by the intersection between the hull and the water surface. According to Eda, this line is not straight when under significant roll, as well as the direction of the hull-camberline (fore point to aft point) turns negative with positive roll. The speed dependency of these terms is uncertain due to lack of experimental data.

In summary, the coupling terms can be evaluated as shown in table 2.

Table 2 Magnitude of Coupling Terms

Coefficient	*Sign*	*Size*
K_p	negative	significant
Y_p	positive	small
N_p	pos/neg	small, depends on trim, location of appendages
Y_φ	pos/neg	small
N_φ	pos/neg	small
$K_{uv}U$	positive	significant, proportional to U
$(K_{ur}+ mz_G)U$	pos/neg	depends on load and trim, proportional to U

Note, that these coefficients are not necessarily comparable if a different model structure is used. Roll-to-yaw and yaw-to-roll coupling coefficients will be remarkably different dependant on the use of geometrical centre (ITTC) or centre of mass [Son & Nomoto, 1982] for origo of the ship-fixed system.

5. ROBUSTNESS TO CHANGES IN ROLL-SWAY-YAW COUPLINGS

Study of the sensitivity to the various parameters is not complicated with access to symbolic manipulation of the system equations. When a particular parameter is investigated, this one is retained as a symbol, while all others are substituted with their numeric values. As an example, with z_G as a parameter, the E, F, and G matrices are, at ship speed 9 m/s :

$$E = \begin{bmatrix} 0.752*10^6 & 0.187*10^6 & -0.359*10^6*(zG-0.82) & 0 & 0 \\ -1.751*10^6 & 62.4*10^6 & 0 & 0 & 0 \\ -0.359*10^6*(zG+0.82) & 0 & 4.174*10^6 & 0 & 0 \\ 0 & 0 & 0 & 1 & 0 \\ 0 & 0 & 0 & 0 & 1 \end{bmatrix}$$

$$F = \begin{bmatrix} -0.106*10^6 & -2.05*10^6 & 0 & -6.0*10^3 & 0 \\ -0.828*10^6 & -3.15*10^7 & 0 & -0.648*10^6 & 0 \\ +0.833*10^5 & 3.23*10^6*(zG-0.28) & -0.640*10^6 & -2.83*10^6 & 0 \\ 0 & 0 & 1 & 0 & 0 \\ 0 & 1 & 0 & 0 & 0 \end{bmatrix}$$

$$G = \begin{bmatrix} +0.105\,10^6 \\ -2.47\,10^6 \\ -0.126\,10^6 \\ 0 \\ 0 \end{bmatrix} \qquad (32)$$

Model uncertainty to changes in roll-sway-yaw coupling term parameters are characterized through

a) Bode or phase-gain plots in r/δ and φ/δ for the envelope of parameters and
b) Pole and zero locations.

Robustness in performance and stability against parameter changes are quantified by

a) Reduction ratio in roll angle and roll velocity and
b) Stability margins for the multivariable system.

Roll reduction ratios are calculated as shown above. Stability margins for the multivariable system are examined through phase-gain plots for the loop transfer operator and by closed

loop pole locations.

5.1 Envelope of parameter variation.

Looking at the parameters for the naval multipurpose vessel, it was chosen to make the envelope of parameter changes by the following span of the individual parameters:

U	*5 to 15 m/s*	
Kp	*-0.3 to -1.3 10^6 Nm/(rad/s)*	*The range in K_p corresponds to natural damping ratios ς from 0.04 to 0.18.*
Np	*-3 to +2 10^6 Nm/(rad/s)*	*The range in N_p was found by considering an increase in ς from 0.1 to 0.2 obtained by bilge keels positioned at different places along the hull.*
z_G	*-2.0 to -0.75 m*	*The range in z_G corresponds to changes in loadings which may not be realistic for a single naval vessel, but could reflect changes over a series of sisterships.*
K_{uv}		*was not varied because its value can be fairly well estimated from Y_{uv}.*
Y_p		*was not varied independently because of its close correlation to K_p.*

It is noted that this range of variation does not reflect actual data from the series of multipurpose naval vessels.

5.2 Results

Reduction ratio curves for roll angle and roll rate are shown in figures 8 to 11 with varying values of N_p, K_p, z_G, and U_0. They illustrate the performance robustness of the closed loop control system within the envelope of parameter variations. The system's own sensitivity to parameter variation, i.e. the basic model uncertainty, is illustrated by phase-gain plots for the loop operator without controller and varying z_G in figures 12 and 13. The stability robustness of the controller is illustrated in a plot of the loop operator for the system with controller in figure 14.

Performance robustness. The following observations can be made:

In general, roll angle damping is efficient for wave periods (encounter period) from the natural roll period and above. Roll velocity is decreased up to this period and increased above it.

Changes in specific parameters are shown from figures 8 to 11:

N_p Roll angle damping for a 9 second wave changes from 0.36 to 0.50, i.e. a factor 1.4 over the parameter envelope.

U Ship speed variation changes roll angle damping from 0.37 to 0.57 or a factor 1.54 over the parameter envelope for a 9 second wave. Speed scaling is thus not enough to obtain speed independent results. Roll angle damping at vary low frequencies need specific consideration at high speed. The controller and speed scaling structure chosen is not sufficient because roll amplification takes place for wave periods of 16 seconds and above at speeds above 10 m/s.

K_p As it is expected, roll damping ability of the controller is largest when natural roll damping is small. Roll angle damping for a 9 second wave varies from 0.4 to 0.62 or a factor 1.55. When bilge keels are applied, natural roll damping might exceed the range considered, and an even larger change in the rr function could be expected.

z_G Changes in loading condition reflected through changes in z_G - note that GM is unchanged - have a significant effect, not only around a 9 second wave period. The change in |rr| is still 1.3 for a 12 second wave.

These results were partly unexpected because the controller is designed with a large stability margin, yet has fairly high gains.

Model uncertainty. Phase-gain plots in figures 12 and 13 illustrate model uncertainty. They show the ship's transfer functions in heading and roll angles from the rudder, without controller, for varying z_G. For technical reasons, frequencies are not plotted on the figures, but the roll natural eigenfrequency is clearly identified.

As apparent, the yaw control part has no stability problems. The shape of the transfer function is literally unchanged over most of the frequency range when z_G varies. Around the roll natural eigenfrequency, however, a change in cross coupling from roll to yaw motion is clearly seen as z_G changes.

The roll transfer function, by contrast, is clearly affected over most of the frequency range, particularly from zero and up to the roll eigenfrequency.

Stability robustness. The closed loop stability will be a function of the model uncertainty and of the controller design. Figure 14 shows the loop transfer function with controller. The loop transfer function is single input - single output when the loop is opened at the rudder signal level. This enables assessment of total stability robustness in one plot. When z_G is varied, the following is observed: For a nominal z_G of -1.75 m, stability margins are 65 deg in phase angle and 16 dB in gain - a factor 6.3. This is considered more than adequate. When z_G is changes to -2.25 m, however, the system becomes unstable. This is remarkable since each of the loops: yaw control and roll damping are stable if the cross couplings were absent.

By comparison with the roll damping ability, a large numeric value of z_G was found to give

the largest roll damping. However, stability margins of the system are decreased when this happens, and an ultimate limit exists where the system becomes unstable. It has thus been demonstrated that the effects of cross couplings are significant in both roll damping ability and in stability of the RRD-autopilot system.

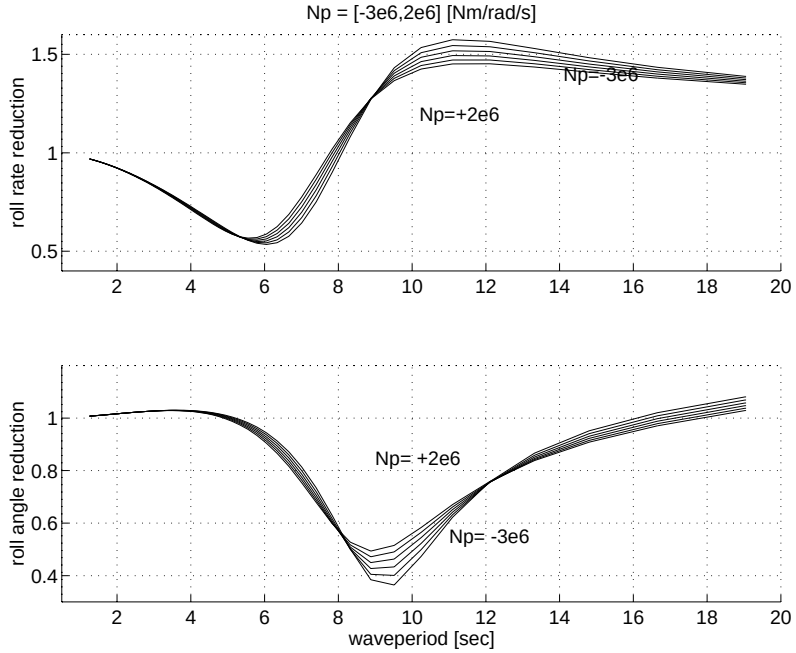

***Figure 8**: Roll reduction ratio for roll rate and roll angle as function of wave period. The roll-rate to yaw moment coefficient N_p is varied.*

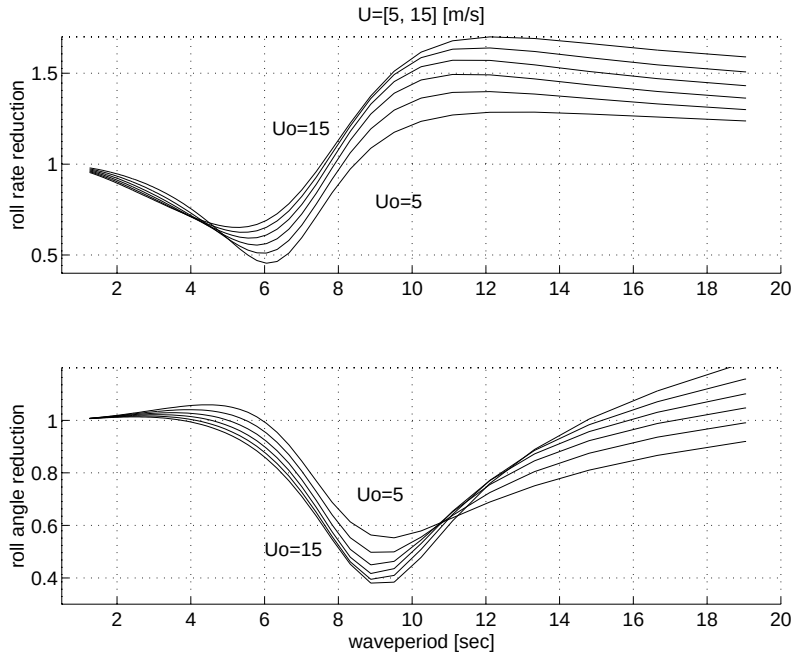

***Figure 9** Roll reduction ratio for roll rate and roll angle as function of wave period. Ship speed is varied from 5 m/s to 15 m/s.*

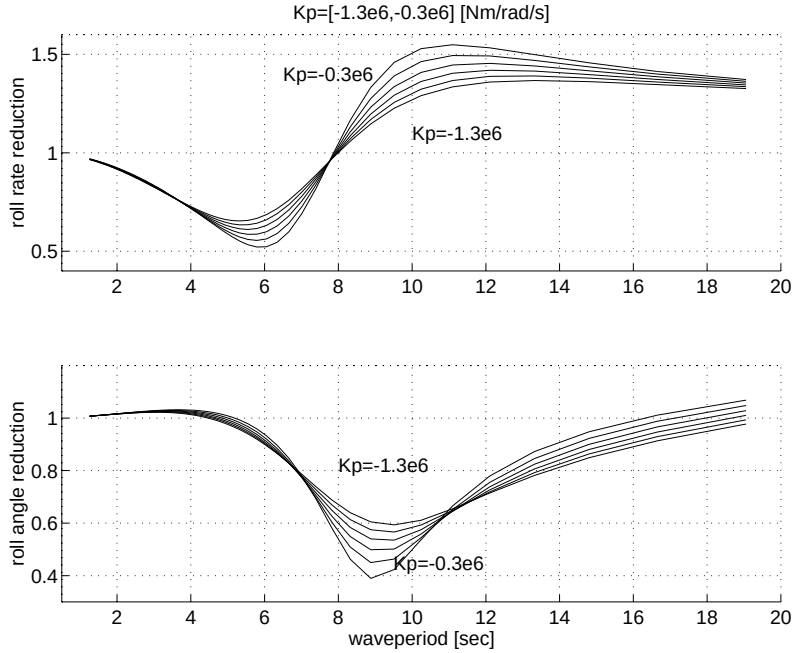

Figure 10 *Roll reduction ratio for roll rate and roll angle as functions of wave period. Variation in roll damping coefficient K_p. Nominal value is -0.5 10^6 Nm/rad/s.*

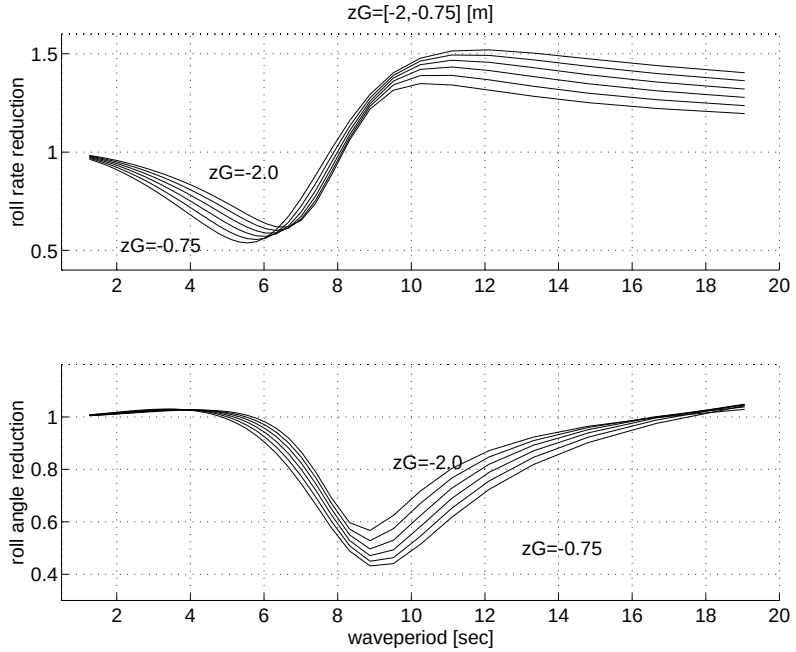

Figure 11 *Roll reduction in roll rate and roll angle as functions of wave period for variation in location of centre of gravity in vertical direction.*

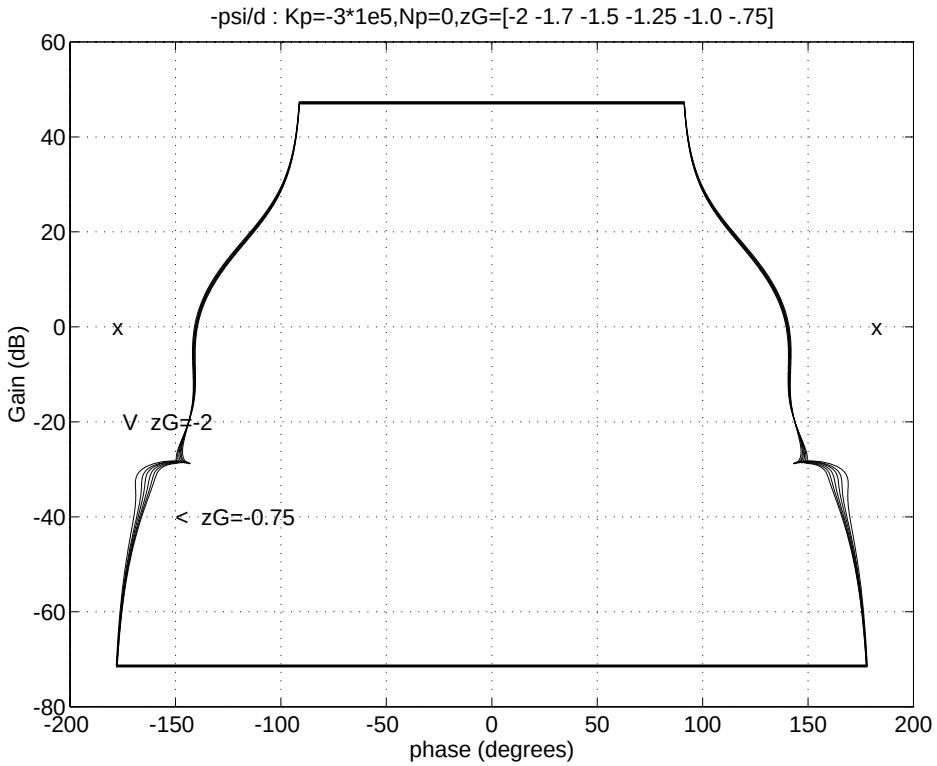

Figure 12 *Phase-gain plot of the open loop heading transferfunction - $\psi(s)/\delta(s)$ for variation in z_G..*

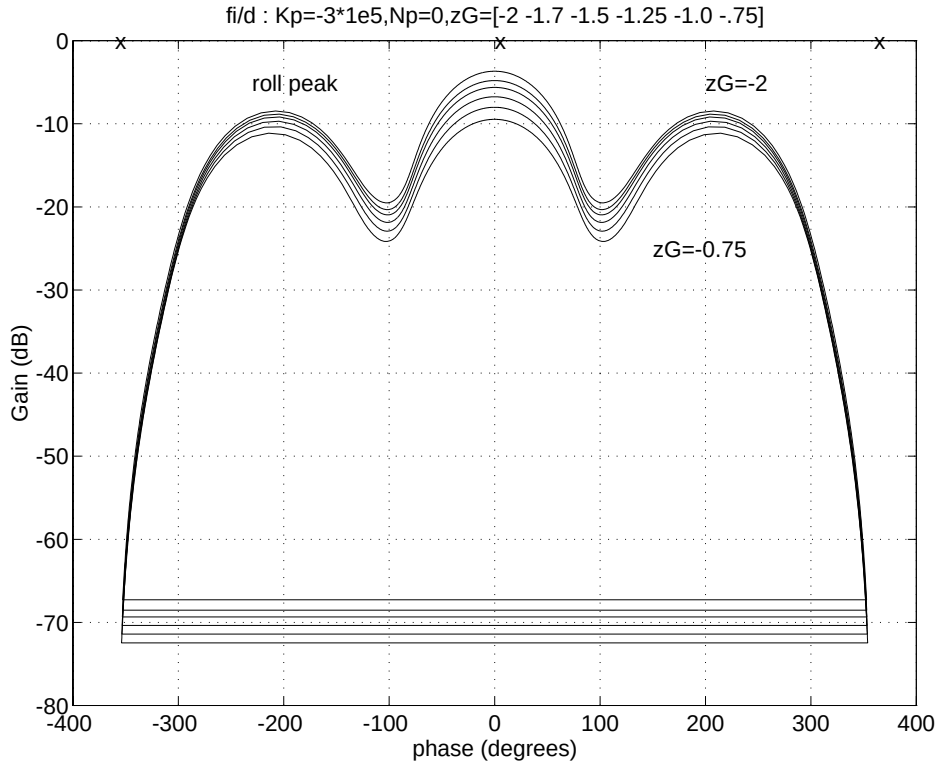

Figure 13 *Phase-gain plot of the open loop roll transfer function $\varphi(s)/\delta(s)$ for variation in z_G. Increasing| zG| gives less stability margin.*

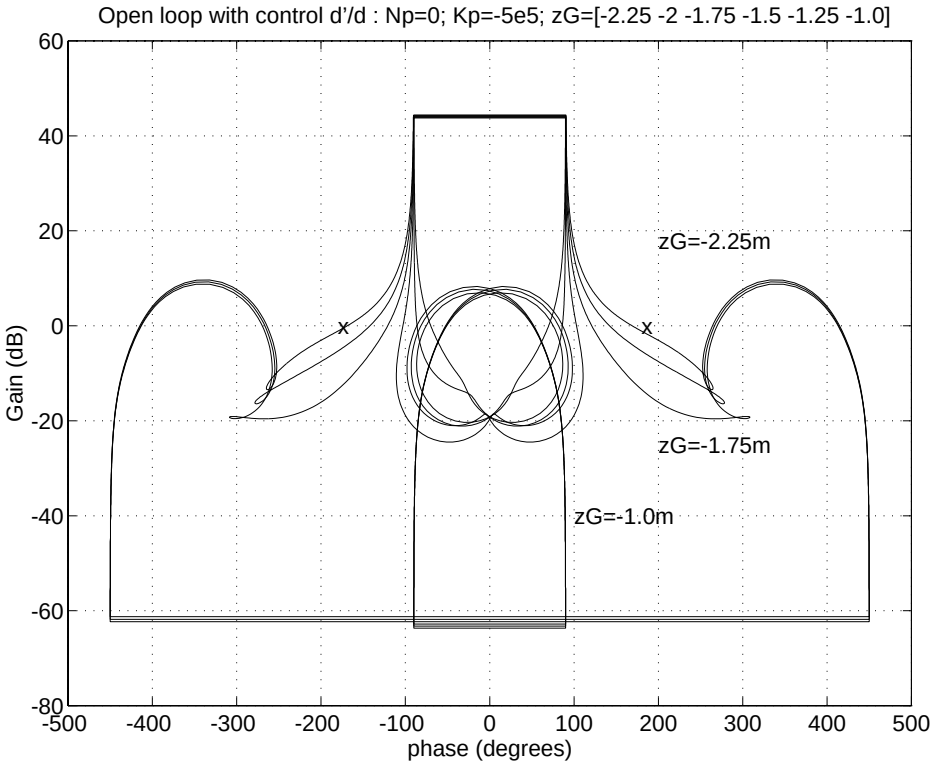

Figure 14 *Phase-gain plot of the loop transfer function with nominal controller. Loop stability is clearly affected when z_G is varied, and at 2.25 m, the system becomes unstable.*

6. SUMMARY

Robustness properties of rudder-roll-damping autopilot control have been treated. Recent experiences with a series of sister vessels showed roll damping on the first to be very satisfactory, whereas performance was much decreased on later vessels where certain changes had been made. Based on this an investigation was made on the effects of changes in appendages like bilge keels and rudders, and in loading conditions. Changes in cross couplings between roll, sway and yaw were identified as a potential source to change both robustness and performance.

One obstacle was the complexity of this problem, another the fact, that these cross-couplings have only been sparsely treated in the literature. Symbolic mathematical manipulation was introduced to analyze the hydrodynamic equations and provide knowledge about relations between hydrodynamic parameters and control dynamics of the RRD autopilot problem.

A structured uncertainty model for use in robust RRD systems design was given, and it was shown that changes in coupling terms between steering and roll can change the roll damping ability significantly. The effects of uncertainty within given bounds were illustrated on an RRD - heading controller using data from a naval multipurpose vessel. The controller chosen was scaled with ship speed, but was not otherwise adapted to parameter changes. The structure was idealized state feedback. It was shown that realistic changes in coupling terms and other uncertain parameters can give important changes to the control dynamics, and as a consequence, significant changes in the performance of the multivariable control system. It was noted that these results are valid for a fairly general class of state constant controllers but that the robustness results can not be directly generalized to self adaptive methods.

The paper is believed to contribute by advising ways to access the effects of coupling term changes on RRD control and by showing that changes in roll reduction capability may be significant for changes in coupling parameters. The inclusion of a complete parameterized model that can be used for comparison of methodology in RRD design is also believed to be useful.

7. ACKNOWLEDGEMENTS

The authors are indebted to the Danish Naval Material Command and the Danish Maritime Institute for the permission use and publish the estimated parameters for the multipurpose vessel.

Part of this research work was done under contract 26-1830 with the Danish Research Council. This support is gratefully acknowledged.

8. REFERENCES

van Amerongen, J.; van der Klugt, P.G.M.; Pieffers, J.B.M.: Rudder-roll stabilization, Controller Design and Experimental Results. *Proc. 8th SCSS*, den Hague, NL, 1987.

Baitis, A.E., Woolaver, D.A., & Beck, T.A.: Rudder roll stabilization for coastguard cutters and frigates. *Naval Engineering Journal*, 1983.

Blanke, M: *Ship Propulsion Losses Related to Automatic Steering and Prime Mover Control*. Ph.D. Thesis, Technical University of Denmark, Lyngby, Denmark, 1982.

Blanke, M.; P. Haals, P.& K.K. Andreasen: Rudder-roll damping experience in Denmark. *Proc. IFAC workshop on Control Applications in Marine Systems, CAMS '89:* Lyngby, Denmark, 1989.

Christensen, A.: *Models of Control Design - Modelling and Validation in Ship Control*, Ph.D. Thesis, Institute of Automatic Control Systems, Technical University of Denmark, Lyngby, Denmark, 1992.

Christensen, A.: Prospects in Symbolic Processing for modelling in Control System Design, *Proc. 12. IFAC World Congress*, Sidney, Aus. 1993

Comstock, J.P. (ed.): *Principles of Naval Architecture*, Society of Naval Architecture and Marine Engineers, New York, 1967

Eda, H.: Rolling and steering performance of highspeed ships - simulation studies of yaw-roll coupled instabilities. *Proc. 13. Symposium on Naval Hydrodynamics*, 1980

Källström, C.G.: Control of yaw and roll by a rudder/fin stabilization system. *Proc. 6th SCSS*, Ottawa Canada 1981.

Källström, C.G. & W.L.Schultz: An integrated rudder control system for roll damping and course maintenance. *Proc. 9th Ship Control Systems Symposium*, Washington, USA, 1989.

van der Klugt, P.G.M: Rudder roll stabilization on board the HMS Karel Doorman. *Journal of Naval Engineering*, Dec. 1991.

Norrbin, Nils H.: Theory and observations on the use of a mathematical model for ship manoeuvring in deep and confined waters. *Publications of the Swedish state Shipbuilding Experimental Tank* no 68, Göteborg, Sweden, 1971

Roberts, G.N.: Ship roll damping using rudder and stabilising fins. *Proc. IFAC workshop on Control Applications in Marine Systems, CAMS´92*, Genova, Italy, 1992.

Son, K.H., K. Nomoto: On the Coupled Motion of Steering and Rolling of a High-speed Container Ship, *Journal of Naval Architecture and Ocean Engineering*, vol. 20, 1982.

APPENDIX A. INVERSE OF THE INERTIA MATRIX

The advent of effective tools for symbolic mathematical calculations have made many tedious calculations obsolete and it is most appropriate to keep machine generated expressions within the symbolic tools. The inverse of the inertia matrix is an example on this, and the expression below is considered too large to enable effective use by manual means. Nevertheless, for the sake of completeness, and to enable the reader to make an independent judgement of some of the statements made in the paper, the analytical inverse is reproduced below.

The inertia matrix is

$$E = \begin{bmatrix} m - Y_{\dot{v}} & m\,x_G - Y_{\dot{r}} & -Y_{\dot{p}} - m\,z_G \\ -N_{\dot{v}} + m\,x_G & I_{zz} - N_{\dot{r}} & -N_{\dot{p}} \\ -K_{\dot{v}} - m\,z_G & -K_{\dot{r}} & I_{xx} - K_{\dot{p}} \end{bmatrix} \tag{33}$$

The determinant is:

$$\det(E) =$$

$$\begin{aligned} &[\, I_{xx} I_{zz} m - I_{zz} K_{\dot{p}} m - K_{\dot{r}} m N_{\dot{p}} - I_{xx} m N_{\dot{r}} + K_{\dot{p}} m N_{\dot{r}} + \\ &K_{\dot{v}} m N_{\dot{p}} x_G + I_{xx} m N_{\dot{v}} x_G - K_{\dot{p}} m N_{\dot{v}} x_G - I_{xx} m^2 x_G^2 + \\ &K_{\dot{p}} m^2 x_G^2 - I_{zz} K_{\dot{v}} Y_{\dot{p}} + K_{\dot{v}} N_{\dot{r}} Y_{\dot{p}} - K_{\dot{r}} N_{\dot{v}} Y_{\dot{p}} + \\ &K_{\dot{r}} m x_G Y_{\dot{p}} - K_{\dot{v}} N_{\dot{p}} Y_{\dot{r}} - I_{xx} N_{\dot{v}} Y_{\dot{r}} + K_{\dot{p}} N_{\dot{v}} Y_{\dot{r}} + \\ &I_{xx} m x_G Y_{\dot{r}} - K_{\dot{p}} m x_G Y_{\dot{r}} - I_{xx} I_{zz} Y_{\dot{v}} + I_{zz} K_{\dot{p}} Y_{\dot{v}} + \\ &K_{\dot{r}} N_{\dot{p}} Y_{\dot{v}} + I_{xx} N_{\dot{r}} Y_{\dot{v}} - K_{\dot{p}} N_{\dot{r}} Y_{\dot{v}} - I_{zz} K_{\dot{v}} m z_G + \\ &K_{\dot{v}} m N_{\dot{r}} z_G - K_{\dot{r}} m N_{\dot{v}} z_G + K_{\dot{r}} m^2 x_G z_G + m^2 N_{\dot{p}} x_G z_G - \\ &I_{zz} m Y_{\dot{p}} z_G + m N_{\dot{r}} Y_{\dot{p}} z_G - m N_{\dot{p}} Y_{\dot{r}} z_G - I_{zz} m^2 z_G^2 + \\ &m^2 N_{\dot{r}} z_G^2 \,] \end{aligned} \tag{34}$$

The inverse is:

$$E^{-1} = \frac{1}{\det(E)} *$$

$$\begin{bmatrix} \begin{pmatrix} (I_{xx} I_{zz} - I_{zz} K_{\dot{p}} - K_{\dot{r}} N_{\dot{p}} - I_{xx} N_{\dot{r}} + K_{\dot{p}} N_{\dot{r}}) \\ (K_{\dot{v}} N_{\dot{p}} + I_{xx} N_{\dot{v}} - K_{\dot{p}} N_{\dot{v}} - I_{xx} m x_G + K_{\dot{p}} m x_G + m N_{\dot{p}} z_G) \\ (I_{zz} K_{\dot{v}} - K_{\dot{v}} N_{\dot{r}} + K_{\dot{r}} N_{\dot{v}} - K_{\dot{r}} m x_G + I_{zz} m z_G - m N_{\dot{r}} z_G) \end{pmatrix}^T \\ \\ \begin{pmatrix} -(I_{xx} m x_G) + K_{\dot{p}} m x_G + K_{\dot{r}} Y_{\dot{p}} + I_{xx} Y_{\dot{r}} - K_{\dot{p}} Y_{\dot{r}} + K_{\dot{r}} m z_G) \\ (I_{xx} m - K_{\dot{p}} m - K_{\dot{v}} Y_{\dot{p}} - I_{xx} Y_{\dot{v}} + K_{\dot{p}} Y_{\dot{v}} - K_{\dot{v}} m z_G - m Y_{\dot{p}} z_G - m^2 z_G^2) \\ (K_{\dot{r}} m - K_{\dot{v}} m x_G + K_{\dot{v}} Y_{\dot{r}} - K_{\dot{r}} Y_{\dot{v}} - m^2 x_G z_G + m Y_{\dot{r}} z_G) \end{pmatrix}^T \\ \\ \begin{pmatrix} (-(m N_{\dot{p}} x_G) + I_{zz} Y_{\dot{p}} - N_{\dot{r}} Y_{\dot{p}} + N_{\dot{p}} Y_{\dot{r}} + I_{zz} m z_G - m N_{\dot{r}} z_G) \\ (m N_{\dot{p}} + N_{\dot{v}} Y_{\dot{p}} - m x_G Y_{\dot{p}} - N_{\dot{p}} Y_{\dot{v}} + m N_{\dot{v}} z_G - m^2 x_G z_G) \\ (I_{zz} m - m N_{\dot{r}} + m N_{\dot{v}} x_G - m^2 x_G^2 - N_{\dot{v}} Y_{\dot{r}} + m x_G Y_{\dot{r}} - I_{zz} Y_{\dot{v}} + N_{\dot{r}} Y_{\dot{v}}) \end{pmatrix}^T \end{bmatrix}^T$$

APPENDIX B. DATA FOR MULTIPURPOSE NAVAL VESSEL

Table 3.
Estimated main data for multipurpose naval vessel at project stage. By permission from SMK and DMI.

Main particulars for hull		Value and unit	
Length	L_{pp}	48	[m]
Beam	B	8.6	[m]
Draft	D	2.2	[m]
Mass	m	$359\ 10^3$	[kg]
Displacement	∇	350	[m^3]
Inertia in yaw	I_{zz}	$33.7\ 10^6$	[kg m^2]
Inertia in roll	I_{xx}	$3.4\ 10^6$	[kg m^2]
Ref. speed	U_0	8.23	[m/s]
Centre of gravity coordinates:			
z pos. from ⊠	z_G	-1.75	[m]
x pos. from ⊠	x_G	-3.38	[m]
Rudder data:			
Effective area	A_R	0.73	[m^2]
Lift coefficient	C_L	1.15	
Stall angle	δ_{stall}	30	[deg]
x dist. from ⊠	l_x	-23.5	[m]
z dist. from ⊠	l_z	1.2	[m]
Metacenter	GM	0.776	[m]
Gravity const.	g	9.82	[m/s^2]
Water density	ρ	1025	[kg/m^3]

Table 4.
Estimated hydrodynamic parameters for multipurpose vessel at project stage. Estimates are not based on model tests. By permission from of NMC and DMI.

Coefficient for N	N [Nm]	Coefficient in Y & K	K [Nm]	Y [N]
$\partial v/\partial t$ [m/s^2]	$0.538\ 10^6$	$\partial v/\partial t$ [m/s^2]	$0.296\ 10^6$	$-0.393\ 10^6$
$\partial r/\partial t$ [rad/s^2]	$-28.7\ 10^6$	$\partial r/\partial t$ [rad/s^2]	0	$-1.40\ 10^6$
$\partial p/\partial t$ [rad/s^2]	0	$\partial p/\partial t$ [rad/s^2]	$-0.774\ 10^6$	$-0.296\ 10^6$
$\|u\|v$ [m^2/s^2]	-92000	$\|u\|v$ [m^2/s^2]	9260	-11800
$\|u\|r$ [rad m/s^2]	$-4.71\ 10^6$	ur [rad m/s^2]	$-0.102\ 10^6$	$0.131\ 10^6$
$v\|v\|$ [m^2/s^2]	0	$v\|v\|$ [m^2/s^2]	29300	-3700
$r\|r\|$ [rad^2/s^2]	$-202\ 10^6$	$r\|r\|$ [rad^2/s^2]	0	0
$v\|r\|$ [rad m/s^2]	0	$v\|r\|$ [rad m/s^2]	$0.621\ 10^6$	$-0.794\ 10^6$
$r\|v\|$ [rad m/s^2]	$-15.6\ 10^6$	$r\|v\|$ [rad m/s^2]	$0.142\ 10^6$	$-0.182\ 10^6$
$\Phi\|uv\|$ [rad m^2/s^2]	$-0.214\ 10^6$	$\Phi\|uv\|$ [rad m^2/s^2]	-8400	10800
$\Phi u\|r\|$ [rad^2 m/s^2]	$-4.98\ 10^6$	$\Phi\|ur\|$ [rad^2 m/s^2]	$-0.196\ 10^6$	$0.251\ 10^6$
$\Phi u\|u\|$ [rad m^2/s^2]	-8000	Φuu [rad m^2/s^2]	- 1180	-74
$\|u\|p$ [rad m/s^2]	0	$\|u\|p$ [rad m/s^2]	-15500	0
$p\|p\|$ [rad^2/s^2]	0	$p\|p\|$ [rad^2/s^2]	$-0.416\ 10^6$	0
p [rad/s]	0	p [rad/s]	$-0.500\ 10^6$	0
Φ [rad]	0	Φ [rad]	$0.776\ \rho g\nabla$	0
$\Phi\Phi\Phi$ [rad^3]	0	$\Phi\Phi\Phi$ [rad^3]	$-0.325\ \rho g\nabla$	0